Precision Engineering 35 (2011) 505–511

Contents lists available at ScienceDirect

Precision Engineering

journal homepage: www.elsevier.com/locate/precision

Technical note

Finding the optimal characteristic parameters for 3R pseudo-rigid-body model using an improved particle swarm optimizer

Guimin Chen[a,*], Botao Xiong[a], Xinbo Huang[b]

[a] School of Mechatronics, Xidian University, Xi'an, Shaanxi 710071, China
[b] School of Electronic Information, Xi'an Polytechnic University, Xi'an, Shaanxi 710001, China

ARTICLE INFO

Article history:
Received 26 August 2010
Accepted 7 February 2011
Available online 15 February 2011

Keywords:
Compliant mechanism
Pseudo-rigid-body model
Large deflection
Particle swarm optimizer

ABSTRACT

Compliant mechanisms have been used in many engineering areas where high precision and sensitivity are required. One of the major challenges of designing compliant mechanisms lies in understanding and analyzing the nonlinear deflections of flexible members. The pseudo-rigid-body model (PRBM) method, which simplifies the modeling of the nonlinear deflection by approximating it as motion of rigid links, has been accepted as one of the most important tools for synthesis and analysis of compliant mechanisms. In this paper, a review of various PRBMs is presented. The 3R PRBM whose characteristic parameters are independent of external loads is discussed in detail. For the purpose of finding the optimal set of the characteristic parameters for the 3R PRBM, a six-dimensional objective function is formulated by combining the approximation errors of both tip point and tip slope for the two extreme load cases, i.e., pure moment load and pure vertical force load. A particle swarm optimizer was employed to conduct a continuous search on the objective function. The resulting 3R PRBM with the optimized characteristic parameters shows better performance in predicting large deflections of cantilever beams over the original 3R PRBM.

1. Introduction

Compliant mechanisms, which achieve at least some of their mobility from the deflection of flexible segments rather than from articulated joints only, offer many advantages over their rigid counterparts such as increased precision, ability to be miniaturized (e.g., compliant microelectromechanical systems), and reduced wear, backlash and part number [1]. For this reason, the study and application of compliant mechanisms have gained increasing popularity in recent years, especially in the society for precision engineering. Since many of the flexible segments undergo large deflection, the major challenge of designing compliant mechanisms lies in the difficulty in accurately modeling the nonlinear deflection.

The pseudo-rigid-body model (PRBM) method [1], which simplifies the modeling of the nonlinear deflection by approximating it as motion of rigid links, has been widely accepted as one of the most important tools for synthesis and analysis of compliant mechanisms. The use of PRBM enables us to apply the knowledge available in the field of rigid-body mechanisms to compliant mechanisms. So far, PRBM has been successfully used to identify bistability [2] and tristability [3], characterize dynamic behaviors [4,5], and evaluate workspace [7] of compliant mechanisms.

Although a great deal of work has been done on various PRBMs, there still exists a need for a PRBM that is load-independent and able to approximate exceptionally large deflection. Su [6] recently proposed an interesting PRBM consisting of four rigid links joined by three torsion springs (as shown in Fig. 1), which addresses this need well. This PRBM will be referred to as 3R PRBM in the following. The characteristic radius factors (γ_i, $i=0, 1, 2, 3$, and $\sum_{i=0}^{3}\gamma_i = 1$) of 3R PRBM were optimized by Su [6] using a discrete three-dimensional search routine with grid size of 0.05, and then they were used to compute the optimal values of the stiffness coefficients ($K_{\Theta i}$, $i=1, 2, 3$) by averaging over a wide range of external loads. A detailed description of this process is given in Section 2. It's worth noting that the discrete search and the two-step optimization used by Su [6] might skip better results. Therefore, the current paper employs the particle swarm optimizer [17] (which is a continuous search technique inspired by the swarm behavior of birds flocking, animals herding and fish schooling) to conduct a continuous six-dimensional search for the optimal set of characteristic parameters (including γ_i and $K_{\Theta i}$). The six-dimensional objective function is formulated by combining the approximation errors of both tip point and tip slope for the two extreme load cases, i.e., pure moment load and pure vertical force load. By doing this, we are able to make a comprehensive compromise between approximations of motion and load-deflection characteristics of the 3R PRBM in a single step and guarantee that the globally optimal set of characteristic parameters is achieved.

* Corresponding author. Tel.: +86 138 9280 9948.
E-mail address: guimin.chen@gmail.com (G. Chen).

0141-6359/$ – see front matter © 2011 Elsevier Inc. All rights reserved.
doi:10.1016/j.precisioneng.2011.02.006

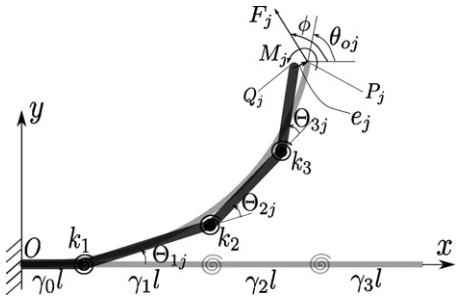

Fig. 1. A 3R PRBM for cantilever beam without inflection.

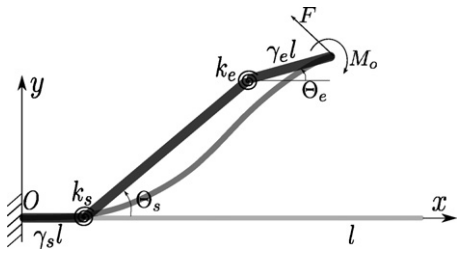

Fig. 3. A 2R PRBM for cantilever beam with an inflection.

The rest of this paper is organized as follows: Section 2 presents a brief summary of various PRBMs for cantilever beams. The fitness function for optimizing the 3R PRBM is formulated in Section 3. Section 4 describes the implementation of the particle swarm optimizer on the fitness function. The optimization results is presented and discussed in Section 5. Section 6 has concluding remarks.

2. Pseudo-rigid-body modeling techniques: a survey

The solutions to the large-deflection equations show that the deflected tip locus for a flexible cantilever beam subject to an end force or an end moment is nearly a circular arc, which makes it possible to approximate the locus by a rigid link rotating around a fixed point. Therefore, Howell and Midha [1] proposed a PRBM that consists of two rigid links joined at a "characteristic pivot" along the beam, as shown in Fig. 2(b). A torsional spring is attached at the characteristic pivot to approximate the stiffness of the beam. This PRBM is referred to as the 1R PRBM in this paper. The 1R PRBM uses three characteristic parameters to identify kinematic and force-deflection characteristics of a flexible segments, namely, the characteristic radius factor (γ), the stiffness coefficient (K_Θ), and the parametric angle coefficient (c_θ). The characteristic pivot is located at a length of γl from the beam tip in its undeflected position, where l is the length of the beam. The spring stiffness of the torsion spring, k, can be expressed as a nondimensional constant

$$k = \gamma K_\Theta \frac{EI}{l} \tag{1}$$

Once γ is determined, the tip locus of the deflected beam can be parameterized in terms of Θ, the pseudo-rigid-body angle. It was found that there is a nearly linear relationship between the beam tip angle θ_o and Θ, which can be approximately expressed as

$$\theta_o = c_\theta \Theta \tag{2}$$

When a force F is applied, γ, K_Θ and c_θ can be represented as functions of the force direction angle ϕ but $\gamma = 0.85$, $K_\Theta = 2.65$ and $c_\theta = 1.24$ are usually chosen for simplicity. For a pure moment load, it was found that $\gamma = 0.7346$, $K_\Theta = 2.0643$, and $c_\theta = 1.5164$. The existence of c_θ in the 1R PRBM complicates modeling of potential energy stored in flexible members subject to combined loads [5].

Saxena and Kramer [8] modified the 1R PRBM by replacing the two rigid links with axially compressible links for the purpose of modeling flexible beams subject to combined loads. The use of axially compressible links accounts for the displacement of the characteristic pivot and the decrease in the characteristic radius, thus improves the approximation accuracy of the PRBM. Dado [9] proposed a variable parametric PRBM based on the 1R PRBM, whose parameters are determined by using two correlation functions between the applied end load and the characteristic parameters. These two PRBMs are effective in determining the path, but require iteration when the load actuated on flexible members varies during the motion of a compliant mechanism, since the parameters for the PRBMs are not load-independent.

Lyon et al. [10] classified combined force and moment loading conditions into three cases (i.e., the force and moment are in the same direction, the force and moment are in opposite directions and no inflection is produced, and the force and moment are in opposite directions and an inflection is produced), and correspondingly developed three PRBMs. These PRBMs are valuable in a few cases but limited because the loading conditions of the flexible segments in compliant mechanisms may be different at different positions [3].

Kimball et al. [11] presented a PRBM consisting of three rigid links joined by two torsion springs, which is able to model a flexible beam with an inflection point, as shown in Fig. 3. This model can be considered as a 2R PRBM. By specifying a linear relationship between the two joint angles, namely, $\Theta_s = c\Theta_e$, where c is a constant, the model was reduced to a single degree-of-freedom model. An optimization algorithm was employed to determine the parameters γ_s, γ_e and c. As a result, these parameters, which were given as functions of two non-dimensional load-parameters, can vary significantly depending on the loading condition. A similar PRBM with $\gamma_s = \gamma_e$ was studied by Lyon and Howell [12].

As aforementioned, the load actuated on a flexible member can vary significantly during the motion of a compliant mechanism, thus a PRBM with the characteristic parameters remaining constant regardless of the change of load modes can be very useful in the design and analysis of compliant mechanisms. Therefore, a new 3R PRBM whose characteristic radius factors and stiffness coefficients are independent of external loads was proposed by Su [6]. This PRBM is able to accurately approximate very large deflection over a wide range of load modes when there is no inflection point in

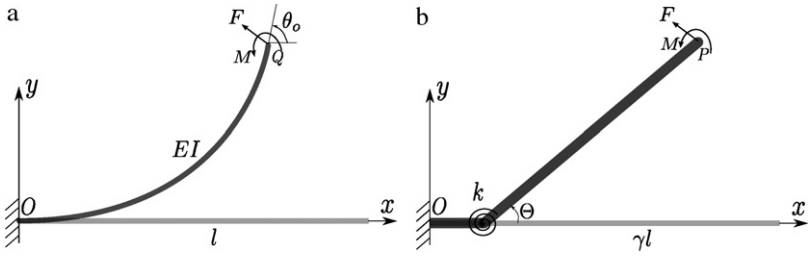

Fig. 2. (a) A cantilever beam subject to a combined end force and moment at the free end and (b) its 1R PRBM.

Table 1
The characteristic parameters given in Ref. [6].

	γ_0	γ_1	γ_2	γ_3	$K_{\Theta 1}$	$K_{\Theta 2}$	$K_{\Theta 3}$
Characteristic parameters in Ref. [6]	0.1	0.35	0.4	0.15	3.51	2.99	2.58

the deflected beam. The characteristic parameters for the 3R PRBM were determined using the following process [6]:

- Suppose that each of γ_i (i = 0, 1, 2, 3) falls in the range of [0.05,0.5], which is divided evenly with step size of 0.05. Repeatedly pick a set of γ_i that satisfies $\sum_{i=0}^{3}\gamma_i = 1$, and compute corresponding sets of $K_{\Theta i}$ (i = 1, 2, 3) based on the load-deflection characteristics of the model for two extreme load cases, i.e., pure moment load and pure vertical force load, respectively. Then the set of γ_i that has the minimum difference between the sets of $K_{\Theta i}$ for the two extreme load cases was selected as the best.
- For the purpose of finding a set of $K_{\Theta i}$ that fits all load modes well, $K_{\Theta i}$ should be computed by averaging over a wide range of external loads for the optimal set of γ_i. It was found that $K_{\Theta i}$ are slightly correlated to force direction angle ϕ. Therefore, the averaging was made over $\kappa \in [0,25]$ with $\phi = \pi/2$, where κ is the load ratio defined as

$$\kappa = \frac{M^2}{2FEI} \tag{3}$$

Table 1 lists the optimized characteristic parameters obtained in Ref. [6], where the relationship between the stiffness coefficients ($K_{\Theta i}$) and the spring stiffnesses (k_i) of the torsion springs can be expressed as

$$K_{\Theta i} = \frac{l}{EI}k_i, \quad i = 1, 2, 3 \tag{4}$$

Although the 3R PRBM is relatively complex as compared to the other PRBMs aforementioned, it offers several advantages such as decoupling of the characteristic parameters and loads, and elimination of the parametric angle coefficient c_θ.

Considering that the discrete search and the two-step optimization incorporated in Ref. [6] may skip better results for the 3R PRBM, we employ in this paper, a population-based searching technique called particle swarm optimizer, to conduct a six-dimensional continuous search for the optimal set of characteristic parameters. The six tuning variables include γ_1, γ_2, γ_3, $K_{\Theta 1}$, $K_{\Theta 2}$, and $K_{\Theta 3}$ (note that $\gamma_0 = 1 - \gamma_1 - \gamma_2 - \gamma_3$). We assume that there is no inflection point in the deflected beam as Su did in Ref. [6]. In the following section, a six-dimensional objective function for finding the optimal set of characteristic parameters for the 3R PRBM is formulated.

3. Problem formulation

For different load modes, the most suitable characteristic parameters for PRBMs might change significantly. The objective of this paper is to find an optimal set of the characteristic parameters (including γ_1, γ_2, γ_3, $K_{\Theta 1}$, $K_{\Theta 2}$ and $K_{\Theta 3}$) for the 3R PRBM that fits all load modes well. As discussed in Ref. [6] two load modes, i.e., the pure end moment load and the pure vertical end force load, can represent two extreme load cases for determining the characteristic parameters (since the two load cases represent the extreme cases, the approximation error for other load modes can be guaranteed to be small). Therefore, the problem may be formally stated as follows: Find the values of the characteristic parameters, which minimize the approximation errors of the 3R PRBM for the two extreme load cases.

For convenience, the actual tip deflections calculated using the analytic methods are denoted by x_{pj}/l, y_{pj}/l (coordinates of tip point "P_j" expressed in nondimensional form) and θ_{oj}, while the approximate tip deflections calculated using the 3R PRBM are denoted by x_{Qj}/l, y_{Qj}/l (coordinates of tip point "Q_j" expressed in nondimensional form) and Θ_{oj}, where j means the jth load step, as will be explained in the following.

It should be noted that our optimization takes the approximation error of the tip slope angle into account for the purpose of taking advantage of one of the aforementioned features of the 3R PRBM namely, elimination the parametric angle coefficient c_θ.

3.1. End moment load

First, we assume a pure moment is applied at the free end of the beam. The moment is increased step by step until the tip slope θ_o reaches $\theta_{o\max}$ ($\theta_{o\max}$ is set to $3\pi/2$ for pure moment load). At the jth load step, by defining a nondimensional moment "index" β_j corresponding to M_j as

$$\beta_j = \frac{M_j l}{EI} \tag{5}$$

where M_j is the applied moment at the jth load step, the actual tip deflection can be calculated as [1]

$$\begin{cases} \theta_{oj} = \dfrac{M_j l}{EI} = \beta_j \\ \dfrac{x_{Pj}}{l} = \dfrac{\sin\theta_{oj}}{\theta_{oj}} \\ \dfrac{y_{Pj}}{l} = \dfrac{1-\cos\theta_{oj}}{\theta_{oj}} \end{cases} \tag{6}$$

On the other hand, the tip deflection predicted by the 3R PRBM for given β_j can be calculated as

$$\begin{cases} \Theta_{oj} = \Theta_{1j} + \Theta_{2j} + \Theta_{3j} \\ \dfrac{x_{Qj}}{l} = \gamma_0 + \gamma_1\cos(\Theta_{1j}) + \gamma_2\cos(\Theta_{1j} \\ \qquad + \Theta_{2j}) + \gamma_3\cos(\Theta_{1j} + \Theta_{2j} + \Theta_{3j}) \\ \dfrac{y_{Qj}}{l} = \gamma_1\sin(\Theta_{1j}) + \gamma_2\sin(\Theta_{1j} + \Theta_{2j}) \\ \qquad + \gamma_3\sin(\Theta_{1j} + \Theta_{2j} + \Theta_{3j}) \end{cases} \tag{7}$$

where, $\Theta_{1j} = \beta_j/K_{\Theta 1}$, $\Theta_{2j} = \beta_j/K_{\Theta 2}$, and $\Theta_{3j} = \beta_j/K_{\Theta 3}$.

Correspondingly, we define the approximation error of 3R PRBM for end moment load (e_M) as the sum of square errors between the predicted and the actual tip deflections at each load step (totally 50 load steps):

$$e_M = \sum_{j=1}^{50}\left[\left(\frac{x_{Pj}}{l} - \frac{x_{Qj}}{l}\right)^2 + \left(\frac{y_{Pj}}{l} - \frac{y_{Qj}}{l}\right)^2 + (\theta_{oj} - \Theta_{oj})^2\right] \tag{8}$$

3.2. Vertical end force load

We use the elliptic integral method [1] to solve the actual tip deflections when a vertical end force is actuated. Because it is not convenient to calculate the tip deflections with given end forces, we use given tip slope at jth load step, θ_{oj} ($\theta_{o\max}$ is set to $9\pi/20$ because $\theta_{o\max} < \pi/2$ for a vertical end force load), to solve for the corresponding force F_j (or nondimensionalized as α_j). The elliptic integral solution is presented in the following and the detailed derivation can be found in Ref. [1].

The force at the jth load step can be expressed as

$$F_j = \frac{\alpha_j^2 EI}{l^2} \tag{9}$$

where α_j is the nondimensional force index expressed as

$$\alpha_j = \mathcal{F}(t_j) - \mathcal{F}(\chi_j, t_j) \tag{10}$$

where

$$\chi_j = \arcsin\sqrt{\frac{1}{1+\lambda_j}} \tag{11}$$

and

$$t_j = \sqrt{\frac{1+\lambda_j}{2}} \tag{12}$$

where

$$\lambda_j = \sin\theta_{oj} \tag{13}$$

Then, the tip point (normalized values) is given by:

$$\begin{cases} \dfrac{x_{Pj}}{l} = \dfrac{1}{\alpha_j}[\sqrt{2(1+\lambda_j)}\cos\chi_j] \\ \dfrac{y_{Pj}}{l} = \dfrac{1}{\alpha_j}[\mathcal{F}(t_j) - \mathcal{F}(\chi_j, t_j) + 2\mathcal{E}(\chi_j, t_j) - 2\mathcal{E}(t_j)] \end{cases} \tag{14}$$

In Eqs. (10)and (14), $\mathcal{F}(\,)$ and $\mathcal{E}(\,)$ represent the elliptic integrals of the first and second kinds, respectively.

Given the vertical force at the jth load step (α_j) on the free end of the 3R PRBM, the torques at the three pin joints can be expressed as

$$\begin{cases} \tau_1 = k_1\Theta_1 = F_j l[\gamma_3\ \cos(\Theta_{1j}+\Theta_{2j}+\Theta_{3j}) \\ \qquad +\gamma_2\ \cos(\Theta_{1j}+\Theta_{2j}) + \gamma_1\cos(\Theta_{1j})] \\ \tau_2 = k_2\Theta_2 = F_j l[\gamma_3\ \cos(\Theta_{1j}+\Theta_{2j}+\Theta_{3j}) \\ \qquad +\gamma_2\ \cos(\Theta_{1j}+\Theta_{2j})] \\ \tau_3 = k_3\Theta_3 = F_j l\gamma_3\ \cos(\Theta_{1j}+\Theta_{2j}+\Theta_{3j}) \end{cases} \tag{15}$$

which can be rewritten in a nondimensional form as

$$\begin{cases} \dfrac{K_{\Theta1}\Theta_1}{\alpha_j^2} = \gamma_3\cos(\Theta_{1j}+\Theta_{2j}+\Theta_{3j}) + \gamma_2\ \cos(\Theta_{1j}+\Theta_{2j}) \\ \qquad\qquad +\gamma_1\cos(\Theta_{1j}) \\ \dfrac{K_{\Theta2}\Theta_2}{\alpha_j^2} = \gamma_3\cos(\Theta_{1j}+\Theta_{2j}+\Theta_{3j}) + \gamma_2\ \cos(\Theta_{1j}+\Theta_{2j}) \\ \dfrac{K_{\Theta3}\Theta_3}{\alpha_j^2} = \gamma_3\cos(\Theta_{1j}+\Theta_{2j}+\Theta_{3j}) \end{cases} \tag{16}$$

For a given set of (γ_1, γ_2, γ_3, $K_{\Theta1}$, $K_{\Theta2}$, $K_{\Theta3}$), Eq. (15) can be solved numerically (using, e.g., the "fsolve" function in MATLAB) to obtain Θ_{1j}, Θ_{2j}, and Θ_{3j} by assuming $l = 1$ without loss of generality. Then, the tip deflection predicted by the 3R PRBM can be expressed as

$$\begin{cases} \Theta_{oj} = \Theta_{1j} + \Theta_{2j} + \Theta_{3j} \\ \dfrac{x_{Qj}}{l} = \gamma_0 + \gamma_1\cos(\Theta_{1j}) + \gamma_2\cos(\Theta_{1j}+\Theta_{2j}) \\ \qquad +\gamma_3\cos(\Theta_{1j}+\Theta_{2j}+\Theta_{3j}) \\ \dfrac{y_{Qj}}{l} = \gamma_1\sin(\Theta_{1j}) + \gamma_2\sin(\Theta_{1j}+\Theta_{2j}) \\ \qquad +\gamma_3\sin(\Theta_{1j}+\Theta_{2j}+\Theta_{3j}) \end{cases} \tag{17}$$

Then, we define the approximation error of the 3R PRBM for vertical end force load (e_F) as the sum of square errors between the predicted and the actual tip deflections at each load step (totally 50 load steps):

$$e_F = \sum_{j=1}^{50}\left[\left(\frac{x_{Pj}}{l} - \frac{x_{Qj}}{l}\right)^2 + \left(\frac{y_{Pj}}{l} - \frac{y_{Qj}}{l}\right)^2 + (\theta_{oj} - \Theta_{oj})^2\right] \tag{18}$$

3.3. Formulation of fitness function for the 3R PRBM

By adding the two approximation errors associated with the two extreme load cases (i.e., pure moment load and pure vertical force load), a fitness function can be formulated as a minimization objection function as follows:

$$\begin{array}{ll} \text{Minimize} & \text{Fitness} = e_M + e_F \\ \text{subject to} & k_{\Theta1} > 0,\quad k_{\Theta2} > 0,\quad k_{\Theta3} > 0 \\ & \gamma_0 > 0,\quad \gamma_1 > 0,\quad \gamma_2 > 0,\quad \gamma_3 > 0 \\ & \gamma_0 + \gamma_1 + \gamma_2 + \gamma_3 = 1 \end{array} \tag{19}$$

where the optimization parameters include γ_1, γ_2, γ_3, $K_{\Theta1}$, $K_{\Theta2}$, and $K_{\Theta3}$. These parameters define a six-dimensional solution space in which the PSO is employed to search for the optimal solution.

4. The particle swarm optimizer

The particle swarm optimizer (PSO), which was first developed by Kennedy and Eberhart [14] in 1995, is a population-based optimization technique inspired by sociological behavior of bird flocking and fish schooling. In PSO, the population is called the swarm and the individuals are called the particles. Each particle "flies" through the solution space based on the previous experiences of its own and the particles within its neighborhood in search of better solution. Since its first publication, PSO has gained increasing popularity due to its simplicity of implementation and high computational efficiency in performing difficult optimization tasks. It is important to note that PSO was originally designed for real-valued problems, which makes it particularly suitable for optimizing the continuous fitness function defined in Eq. (19) as compared to the genetic algorithm (no binary conversion is required).

PSO starts with generating a population of particles (the swarm) with random positions in the solution space and assigning each particle with a random velocity. Each particle in the swarm represents a possible solution to the problem being solved and each particle's fitness is evaluated according to the fitness function. Assume there are m particles in the swarm. In a d-dimension solution space, the position and velocity of the ith particle ($1 \le i \le m$) at iteration t can be represented as vectors $X_i(t) = [x_{i,1}(t), \ldots, x_{i,1}(t), \ldots, x_{i,d}(t)]^T$ and $V_i(t) = [v_{i,1}(t), \ldots, v_{i,1}(t), \ldots, v_{i,d}(t)]^T$, respectively. Based on fitness evaluation, $P_i(t) = [p_{i,1}(t), \ldots, p_{i,1}(t), \ldots, p_{i,d}(t)]^T$ records the best position obtained by the ith particle, while $G_i(t) = [g_{i,1}(t), \ldots, g_{i,1}(t), \ldots, g_{i,d}(t)]^T$ stores the best position discovered by the whole swarm. The new velocity and position in the jth dimension ($1 \le j \le d$) of particle i for the next iteration are calculated using the following two equations:

$$v_{i,j}(t+1) = wv_{i,j}(t) + c_1\ \text{Rand}()[p_{i,j}(t) - x_{i,j}(t)] + c_2\ \text{Rand}()[g_j(t) - x_{i,j}(t)] \tag{20}$$

$$x_{i,j}(t+1) = x_{i,j}(t) + v_{i,j}(t+1) \tag{21}$$

where w is the inertia weight proposed by Shi and Eberhart [15], Rand() is a function that generates a random number uniformly distributed in the range of [0,1], and c_1 and c_2 denote the acceleration coefficients (usually fixed at 2). There are three independent

Table 2
Optimized characteristic parameters.

	γ_0	γ_1	γ_2	γ_3	$K_{\Theta 1}$	$K_{\Theta 2}$	$K_{\Theta 3}$
Present characteristic parameters	0.125	0.35	0.388	0.136	3.25	2.84	2.95

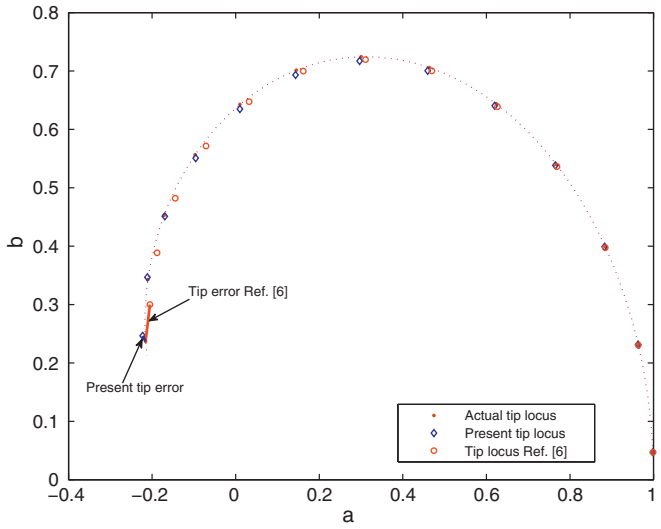

Fig. 4. Comparison of the tip loci of a beam subject to pure moment load predicted by the 3R PRBM in Ref. [6] and present 3R PRBM.

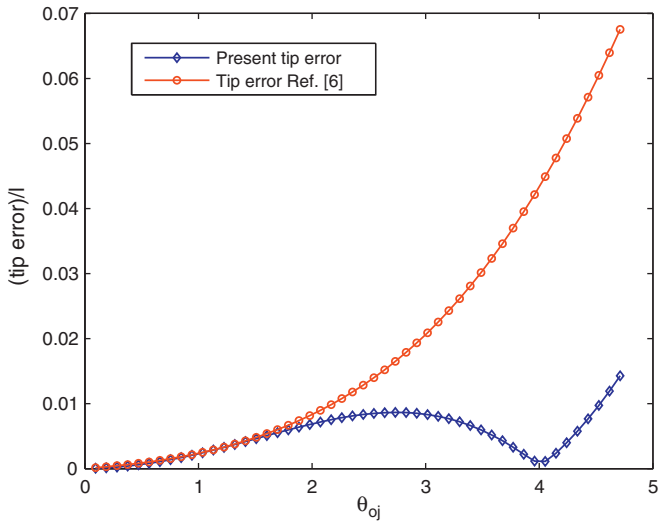

Fig. 5. Comparison of the tip errors of the 3R PRBM in Ref. [6] and present 3R PRBM for a beam subject to pure moment load.

parts in Eq. (20) [14]. The first part is the current velocity weighted by w, which provides the necessary momentum for particles to roam across the search space. The second part, often regarded as the "cognitive" component, represents the personal thinking of each particle and encourages the particles to search around their own best positions found so far. The third part is considered as the "social" component, which represents the collaboration of the particles in the swarm.

In PSO, global exploration is often required during the early stage of the search to allow the particles to survey the full range of the solution space. On the other hand, during the latter stage of the search, when the algorithm has located the area including the optimal solution, local exploitation is crucial for finding the global optima efficiently [15]. The inertia weight (w) offers PSO a convenient way to control between exploration and exploitation. Larger values of the inertia weight always benefit the global exploration, while smaller ones improve the local exploitation. Therefore, a strategy of linearly decreasing the inertia weight was proposed by Shi and Eberhart [16], which initializes the inertia weight to a relatively large value at the beginning of the search and decreases it linearly as the search proceeds. The mathematical representation for linearly decreasing the inertia weight can be given as

$$w = (w_s - w_e) \times \left(\frac{T - t}{T}\right) + w_e \tag{22}$$

where T is the predefined maximum number of iterations, t is the current iteration number, and w_s and w_e are the initial and final values of the inertia weight, respectively (typically $w_s = 0.9$ and $w_e = 0.4$).

In the implementation of PSO for optimizing the fitness function given in Eq. (19), two major changes have been made to improve the efficiency and guarantee the convergence of the algorithm. The first change is that we randomly select a particle from the swarm and initialize it with the characteristic parameters obtained in Ref. [6], as listed in Table 1. The second change is that a nonlinear decreasing strategy [17] is employed instead of the linear one, which can be expressed as

$$w = w_e \times \left(\frac{w_s}{w_e}\right)^{1/(1+10t/T)} \tag{23}$$

Numerical results show that this nonlinear decreasing strategy improves the convergence rates of PSO on a variety of problems [17].

We carry out the optimization with a swarm size of 40 and the maximum number of iterations set to 1000. The optimization results will be presented and discussed in the next section.

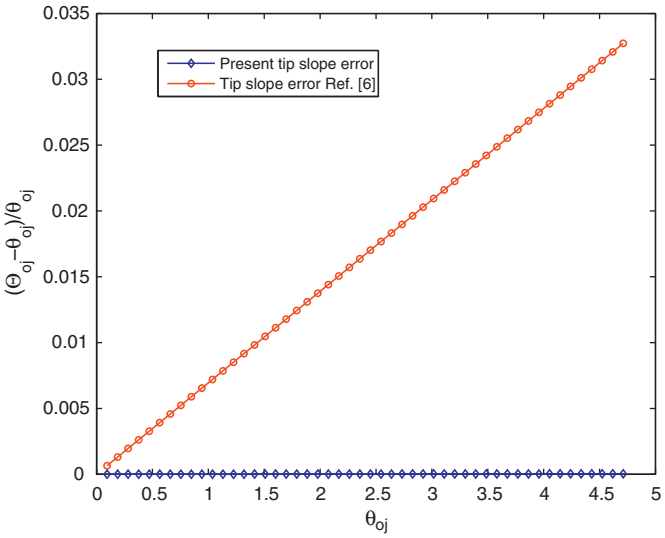

Fig. 6. Comparison of the relative errors of tip slope angle of the 3R PRBM in Ref. [6] and present 3R PRBM for a beam subject to pure moment load.

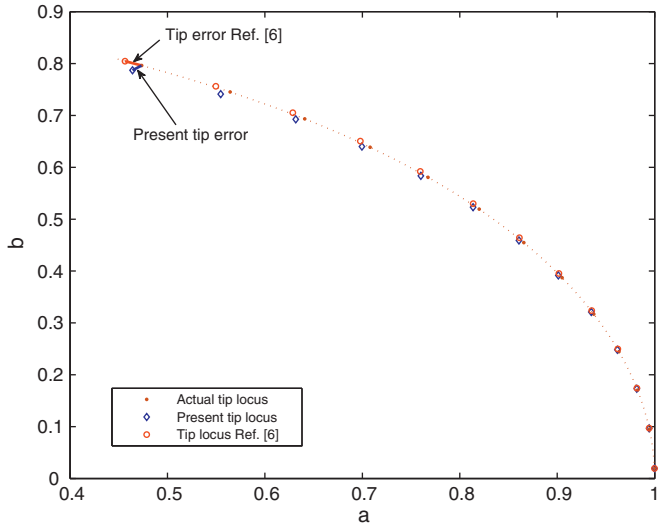

Fig. 7. Comparison of the tip loci of a beam subject to vertical force load predicted by the 3R PRBM in Ref. [6] and present 3R PRBM.

5. Results and discussion

The optimal set of the characteristic parameters found, in this study, by the PSO is listed in Table 2. In the following, the performance of the 3R PRBM with these parameters is evaluated by comparing it with the 3R PRBM parameters given in Ref. [6].

As can be seen from Fig. 4, both of the 3R PRBMs approximate the actual locus well when pure moment is loaded. However, the predicted tip deflection using the 3R PRBM in Ref. [6] lags behind the actual deflection with rather large errors, while present 3R PRBM predicted the tip deflection very well. From Figs. 5 and 6, it can also be concluded that the tip error and the tip slope error of the 3R PRBM in Ref. [6] increase dramatically as the deflection increases, while the corresponding errors associated with present 3R PRBM keeps at a very low level over the whole range of deflection (with the tip error less than 1.5% and the tip slope error of 0.12%). The relative error of tip slope angle with a pure moment load can also be determined mathematically as [6]

$$\left|\frac{1}{K_{\Theta 1}}+\frac{1}{K_{\Theta 2}}+\frac{1}{K_{\Theta 3}}-1\right|=0.12\% \tag{24}$$

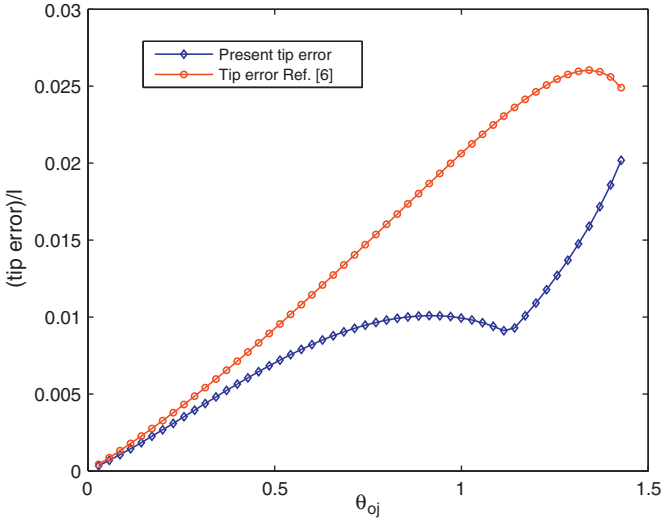

Fig. 8. Comparison of the tip errors of the 3R PRBM in Ref. [6] and present 3R PRBM for a beam subject to vertical force load.

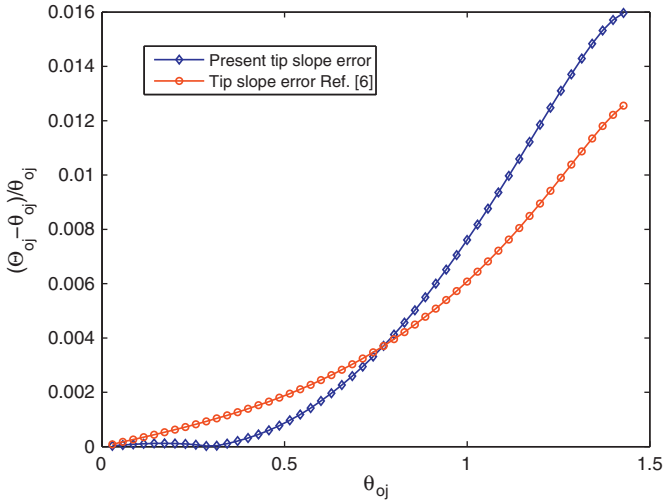

Fig. 9. Comparison of the relative errors of tip slope angle of the 3R PRBM in Ref. [6] and present 3R PRBM for a beam subject to vertical force load.

For vertical end force loads, although the tip locus of present 3R PRBM deviates from the actual locus as the deflection increases, its approximation error is smaller than that of the 3R PRBM in Ref. [6], as can be seen from Fig. 7. The 3R PRBM in Ref. [6] approximates the actual locus well but with relative large overshoot. As to the tip error, present 3R PRBM outperforms the 3R PRBM in Ref. [6] over the whole range of deflection (with errors less than 2%), as shown in Fig. 8. As can be seen from Fig. 9, the relative error of tip slope angle for present 3R PRBM is smaller than that of the 3R PRBM in Ref. [6] when the tip slope is within the range of $0–0.26\pi$, but exceeds when the tip slope is beyond that range. However, the maximum relative slope error is only about 1.6%.

6. Conclusions

For the purpose of finding the optimal set of the characteristic parameters (including γ_1, γ_2, γ_3, $K_{\Theta 1}$, $K_{\Theta 2}$ and $K_{\Theta 3}$) for the 3R PRBM, a six-dimensional objective function is formulated by combining the approximation errors of both tip point and tip slope for the two extreme load cases, i.e., pure moment load and pure vertical force load. An improved particle swarm optimizer was employed to conduct a continuous search on the objective function. The resulting 3R PRBM with the optimized characteristic parameters shows better performance in predicting large deflections of cantilever beams over the 3R PRBM with the parameters presented in Ref. [6].

Acknowledgements

The authors gratefully acknowledge the financial support from the National Natural Science Foundation of China under Grant No. 50805110, the Key Project of Chinese Ministry of Education under No. 109145, and the Fundamental Research Funds for the Central Universities under No. JY10000904010.

References

[1] Howell LL. Compliant mechanisms. New York, NY: Wiley-Interscience; 2001.
[2] Jensen BD, Howell LL. Identification of compliant pseudo-rigid-body mechanism configurations resulting in bistable behavior. ASME J Mech Des 2003;125(4):701–8.
[3] Chen G, Wilcox DL, Howell LL. Fully compliant double tensural tristable micromechanisms (FTTM). J Micromech Microeng 2009;12(2):025011.
[4] Lyon SM, Erickson PA, Evans MS, Howell LL. Prediction of the first modal frequency of compliant mechanisms using the pseudo-rigid-body model. ASME J Mech Des 1999;121(2):309–13.

[5] Yu Y-Q, Howell LL, Lusk C, Yue Y, He M-G. Dynamic modeling of compliant mechanisms based on the pseudo-rigid-body model. ASME J Mech Des 2005;127(7):760–5.
[6] Su H-J. A pseudorigid-body 3R model for determining large deflection of cantilever beams subject to tip loads. ASME J Mech Robot 2009;1(2):021008.
[7] Midha A, Howell LL, Norton TW. Limit positions of compliant mechanisms using the pseudo-rigid-body model concept. Mech Mach Theory 2000;35(1):99–115.
[8] Saxena A, Kramer SN. A simple and accurate method for determining large deflections in compliant mechanisms subjected to end forces and moments. ASME J Mech Des 1998;120(3):392–400.
[9] Dado MH. Variable parametric pseudo-rigid-body model for large-deflection beams with end load. Int J Nonlin Mech 2001;36(7):1123–33.
[10] Lyon SM, Howell LL, Roach GM. Modeling flexible segments with force and moment end loads via the pseudo-rigid-body model. In: Proceedings of the ASME international mechanical engineering congress and exposition, DSC-vol. 69–72. 2000. p. 883–990.
[11] Kimball C, Tsai LW. Modeling of flexural beams subjected to arbitrary end loads. ASME J Mech Des 2002;124:223–35.
[12] Lyon SM, Howell LL. A simplified pseudo-rigid-body model for fixed-fixed flexible segments. In: Proceedings of the ASME design engineering technical conferences. 2002. DETC2002/MECH-34203.
[14] Kennedy J, Eberhart R. Particle swarm optimization. In: Proceedings of IEEE international conference on neural networks. 1995. p. 1942–8.
[15] Shi Y, Eberhart R. A modified particle swarm optimizer. In: Proceedings of IEEE international conference on evolutionary computation. 1998. p. 69–73.
[16] Shi Y, Eberhart R. Empirical study of particle swarm optimization. In: Proceedings of IEEE international congress on evolutionary computation. 1999. p. 101–6.
[17] Chen G, Jia J, Han Q. Study on the strategy of decreasing inertia weight in particle swarm optimization algorithm. J Xi'an Jiaotong Univ 2006;40(1), 53–56, 61 [in Chinese].